Available online at www.sciencedirect.com

ScienceDirect

Procedia Computer Science 218 (2023) 2786–2794

Procedia Computer Science

www.elsevier.com/locate/procedia

International Conference on Machine Learning and Data Engineering

Automatic detection of lung nodule in CT scan slices using CNN segmentation schemes: A study

Seifedine Kadry[a], Enrique Herrera-Viedma[b], Rubén González Crespo[c], Sujatha Krishnamoorthy[d,e,*], and Venkatesan Rajinikanth[f]

[a]*Faculty of Applied Computing and Technology, Noroff University College, Kristiansand, 94612, Norway*
[b]*Andalusian [e]Research Institute in Data Science and Computational Intelligence, University of Granada, Granada, Spain*
[c]*Computer Science Department, School of Engineering and Technology, Universidad Internacional de La Rioja, 26006, Spain*
[d]*Zhejiang Bioinformatics International Science and Technology Cooperation Center, Wenzhou-Kean University, Zhejiang Province, China,*
[e]*Wenzhou Municipal Key Lab of Applied Biomedical and Biopharmaceutical Informatics, Wenzhou-Kean University, Zhejiang Province, China.*
[f]*Department of Electronics and Instrumentation Engineering, St. Joseph's College of Engineering, OMR, Chennai 600119, Tamil Nadu, India*

Abstract

The lung is one of the prime respiratory organs in human physiology, and its abnormality will severely disrupt the respiratory system. Lung Nodule (LN) is one of the abnormalities, and early screening and treatment are necessary to reduce its harshness. The proposed work aims to implement the Convolutional-Neural-Network (CNN) segmentation methodology to extract the LN in various lung CT slices, such as axial, coronal, and sagittal planes. This work consists of the following phases; (i) Image collection and pre-processing, (ii) Ground-truth generation, (iii) CNN-supported segmentation, and (iv) Performance evaluation and validation. In this work, the merit of pre-trained CNN segmentation schemes is verified using (i) One-fold training and (ii) Two-fold training methods. The test images for this study are collected from The Cancer Imaging Archive (TCIA) database. The experimental investigation is executed using Python®, and the outcome of this study confirms that the VGG-SegNet helps to get better values of Jaccard (>88%), Dice (>93%), and Accuracy (>96%) compared to other CNN methods.

Keywords: Lung nodule; CT scan; CNN segmentation; VGG-SegNet; Accuracy; Detection

1. Introduction

The lung is a vital internal organs and is responsible for air exchange between the outer atmosphere and the bloodstream. Therefore, lung disease causes severe respiratory issues, leading to the death of untreated lung disease. In humans, the lung abnormalities are due to; (i) Cancer, (ii) Pneumonia, (iii) Tuberculosis, and (iv) Infectious diseases (ex. COVID119). Cancer is a severe disease and needs appropriate treatment [1].

* Corresponding author. Tel.: +86 133 3691 3765
E-mail address: Sujathaks@ieee.org

10.1016/j.procs.2023.01.250

The incidence rate of cancer is steadily increasing for different reasons, and appropriate identification and treatment are indispensable to treat the disease with appropriate medication. Many cancers can be cured if noticed early and treated successfully. The year 202 report of the World-Health-Organization (WHO) confirms that cancer is one of the leading causes of death worldwide, and it caused nearly 10 million deaths in 2020 alone. This report also confirms that around 2.21 million cases were diagnosed with lung cancer in 2020 alone, and it caused 1.80 million reported deaths worldwide. This holds the leading positing compared to other cancers, such as (i) colon (916 000 deaths), (ii) liver (830 000 deaths), (iii) stomach (769 000 deaths), and (iv) breast (685 000 deaths) [2].

The clinical-level diagnosis of the lung disease is usually achieved by medical imaging schemes, like Computed-Tomography (CT) and radiographs. The visibility of lung's abnormality in CT is clear than X-ray; hence most the lung nodule/cancer detection schemes consider the CT scan slices to achieve a better disease diagnosis. Therefore, a considerable works on the lung nodule detection are executed in the literature using traditional and Convolutional Neural Network (CNN) schemes. Compared to the traditional procedures, the CNN methods helped achieve better detection accuracy during the segmentation task and classification task [3-7].

This work executes a CNN framework to mine and evaluate the nodule in 2D CT scan slices of different planes (axial/coronal/sagittal). The stages of this scheme involve; (i) Clinical grade lung CT collecton, (ii) 3D to 2D translation using ITK-Snap, (iii) Training and testing the CNN segmentation scheme with the test images and binary mask, (iv) Mining the nodule segment from the test images, and (v) Comparing the mined nodule with mask and computing the performance metrics. Based on the achieved values of metrics, such as the Jaccard, Dice, and Accuracy, the merit of this proposal is verified. In this work, a two-fold training process is employed to improve the performance of the CNN segmentation scheme. The initial training is implemented using 200 epochs, and the second training is executed with 100 epochs and the results validates the superiority. A comparative analysis on CNN schemes, like UNet, ResNet, VGG-UNet, SegNet, and VGG-SegNet also presented. The performance metrics realized with VGG-SegNet are better compared to other CNN schemes.

The contributions of this work include;

(i) Implementation of a two-fold training process to improve the CNN segmentation performance
(ii) Comparison of different CNN schemes on the chosen lung CT database

2. Related Research

Detection of the lung abnormality using the traditional and CNN schemes are widely discussed by the researchers. Recently, various CNN segmentation schemes are proposed to extort the required fragment in medical imagery and the summary of few chosen technique is presented in Table 1.

Table 1. Summary of the CNN segmentation methods

Reference	Methodology executed to analyze lung nodule
Rastogi et al. [8]	U-Net scheme based assessment of the colorectal cancer histopathological image is presented with a detailed comparative study.
Kadry et al. [9]	This work presented a comparative analysis of the CNN segmentation schemes using the histology slides.
Kadry et al. [10]	VGG-SegNet based segmentation of the skin cancer image is discussed using the skin melanoma pictures.
Kadry et al. [11]	Extraction and the assessment of the COVID19 lesion from the lung CT images are presented using U-Net scheme.
Daniel et al. [12]	Assessments of the complex fluorescence microscopy image are presented using the improved version of VGG-UNet/VGG-SegNet schemes.
Das [13]	This work presents the UNet-based lung extraction to evaluate the COVID19 infection with ensemble deep features.
Khan et al. [14]	Implementation of the VGG19 based encoder-decoder method is presented to extract and examine the lung nodule.

Kadry et al. [15]	UNet supported mining and examination of the stroke lesion from the 2D brain MRI is presented.
Krishnamoorthy et al. [16]	Implementation of the VGG-UNet to extort the multiple sclerosis lesions in brain MRI is discussed.
Minaee et al. [17]	This work presents a comprehensive review on image segmentation using various CNN segmentation procedures.

The works summarized in Table 1 authenticates the superiority of the CNN schemes. Hence, CNN scheme with a two-fold training is implemented to extract the nodule from the lung CT slices.

3. Methodology

This research proposes a CNN based image mining idea to mine the nodule in CT slices as depicted in Figure 1. After collecting the necessary clinical-grade CT image, 3D to 2D conversion and image resizing are employed for both the test image and the binary mask. These imagery are then chosen to confirm the performance of the CNN scheme using a two-fold training process. First, after mining the nodule in axial-, coronal-, and sagittal planes, an assessment among the binary mask and an extracted nodule is achieved, and then the necessary metrics are calculated.

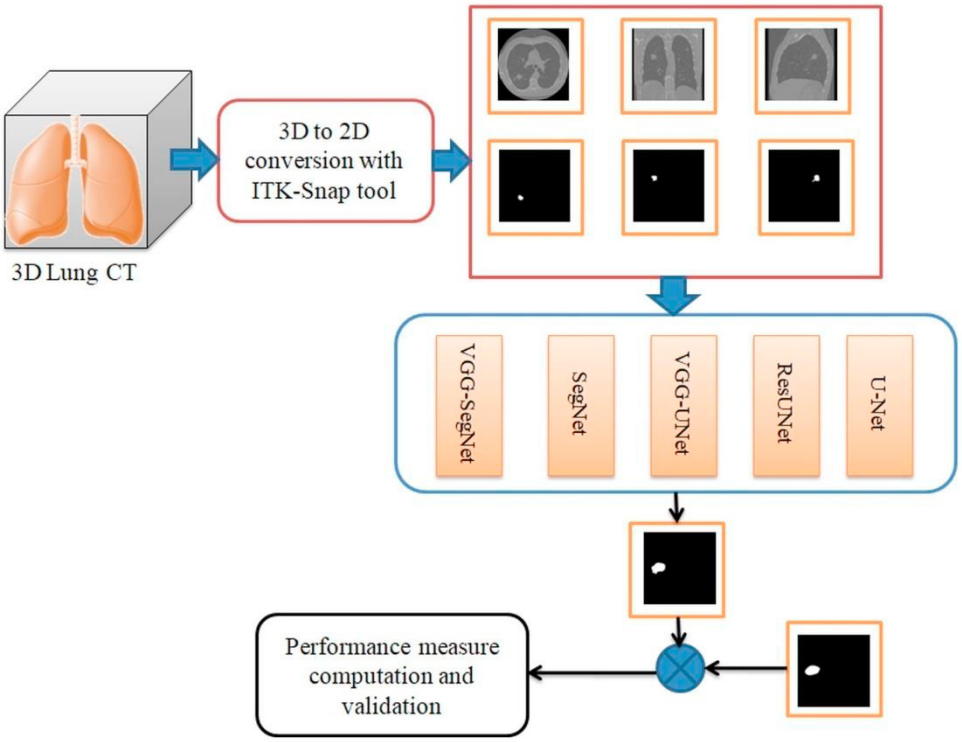

Fig. 1. Block diagram represents the proposed scheme

3.1. Image database

The necessary test pictures and the binary mask are extracted from the TCIA database. In this study, 25 patients' lung images are considered for the study, and from each patient, 20 numbers of 2D CT slices are obtained using ITK-Snap [18,19], and the mined CT slice and its mask image are then resized to $512\times512\times1$ pixels. The sample

images and the related mask (GT) are presented in Figure 2. In this work, 500 numbers of 2D slices are considered for the analysis in every 2D plane, and the attained results are statistically evaluated, and the results are demonstrated.

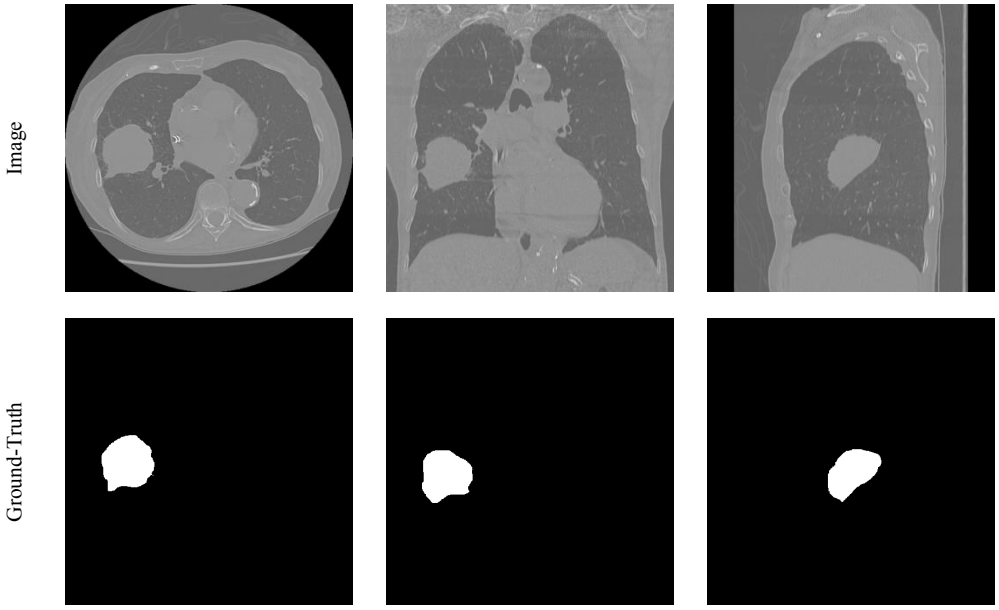

(a) Axial (b) Coronal (c) Sagittal

Fig. 2. Sample test images and the related Ground-Truth

3.2. CNN Segmentation

Due to its improved performance, researchers widely adopted CNN segmentation schemes to mine the nodule in 2D lung CT images. The performance of techniques, like UNet, ResUnet, VGG-UNet, SegNet, and VGG-SegNet, are considered in this work to mine the nodule. In every CNN scheme, the following initial parameters are assigned; Initial weight= ImageNet, Batch value=8, Epochs=200+100, Optimizer=Adam, Pooling=Maximum, Monitoring metric= Accuracy and Loss, Classifier=SoftMax. The outcome of this scheme is then evaluated with the GTand results are verified.

3.3. Validation

The merit of this scheme is verified by a comparative study among nodule and GT; which provides metrics like Jaccard (JA), Dice (DI), Accuracy (AC), Precision (PR), Sensitivity (SE) and specificity (SP). The mathematical expressions for these parameters are presented in [20-22].

4. Results and Discussions

The outcomes of this research are demonstrated in this section. This examination is executed by a computer having Intel i7, 20GB RAM, and 4GB VRAM equipped with Python®.

The CNN scheme is primarily trained using the image and the GT, and then a two-fold learning process is executed as in Figure 3. Fig 3(a) shows the outcome of the training process, and Fig 3(b) shows the convergence of the procedure with respect to epochs. Finally, fig 3(c) presents the predicted nodule.

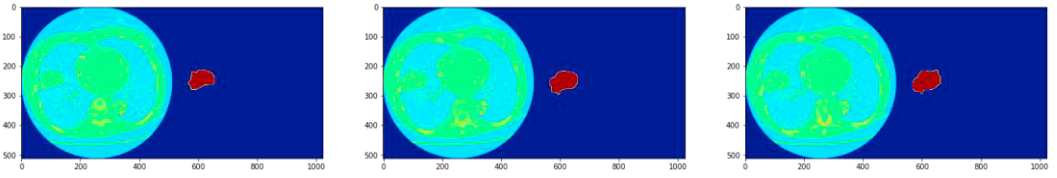

(a) Input image

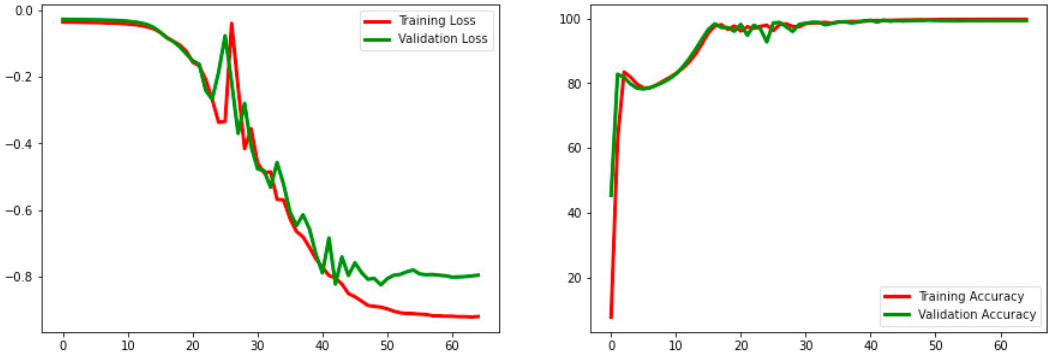

(b) Training and validation convergence

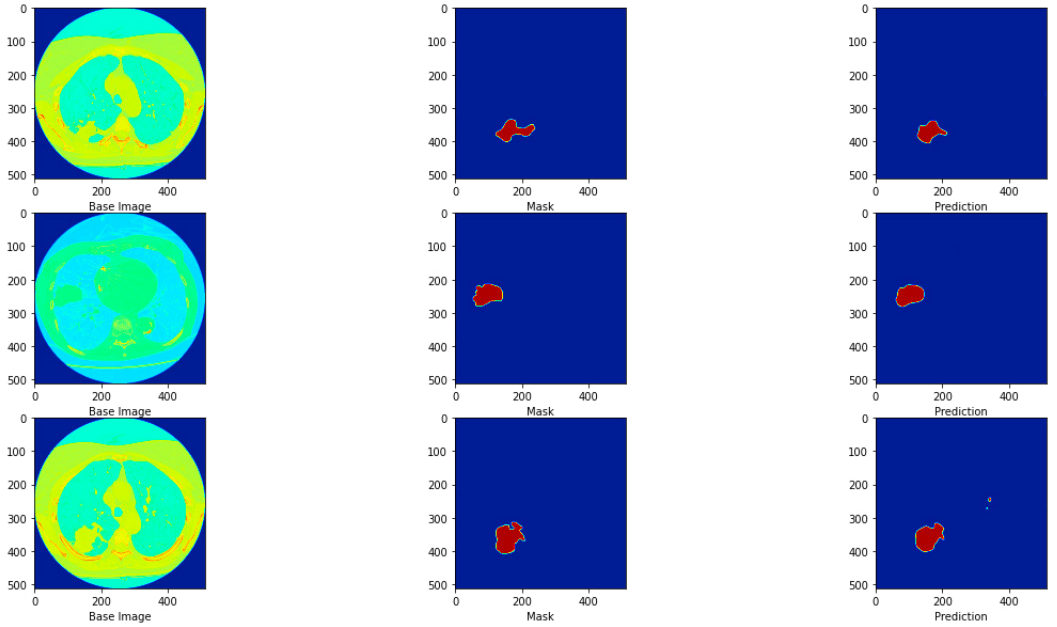

(c) Segmented results

Fig. 3. Results achieved with VGG-SegNet

The binary version of the image is widely adopted in segmentation tasks to compare it with the GT, and the sample binary nodules obtained in this work are shown in Figure 4 and Table 2 shows the computed performance metrics. The average of these values is then considered to verify its performance. Initially, axial-plane images are assessed as discussed, and Table 2 confirms the merit of the CNN. Further, the overall performance of the values available in Table 2 is graphically compared using Glyph-Plot as in Figure 5 also confirms that the achieved results present approximately similar results on the extracted nodule.

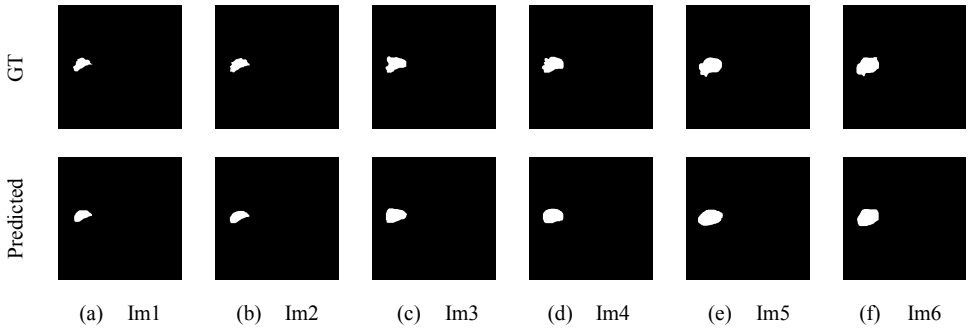

Fig. 4. The GT and the segmented binary image

Table 1. Performance measures computed for sample test images

Image	TP	FN	TN	FP	JA	DI	AC	PR	SE	SP
Im1	2081	255	259608	200	82.0584	90.1451	99.8264	91.2319	89.0839	99.9230
Im2	2477	123	259295	249	86.9428	93.0154	99.8581	90.8657	95.2692	99.9041
Im3	3636	378	257909	220	85.8762	92.4015	99.7719	94.2946	90.5830	99.9148
Im4	3938	302	257608	296	86.8166	92.9431	99.7719	93.0090	92.8774	99.8852
Im5	4854	382	256593	314	87.4595	93.3103	99.7345	93.9241	92.7044	99.8778
Im6	4981	175	256631	357	90.3501	94.9304	99.7971	93.3121	96.6059	99.8611
Average					86.5839	92.7910	99.7933	92.7729	92.8540	99.8943

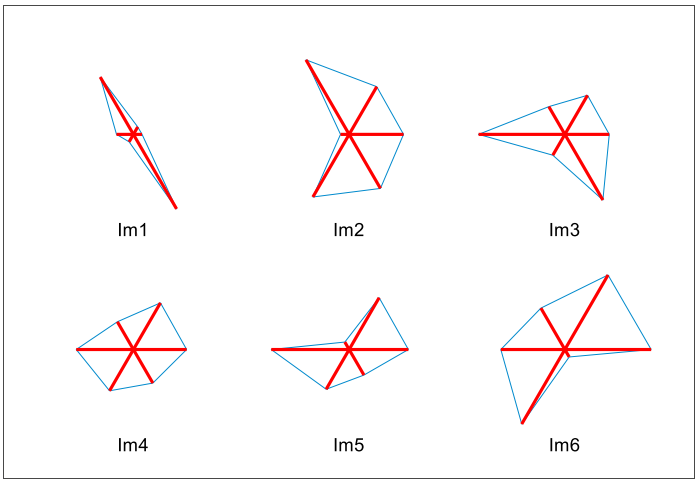

Fig. 5. Glyph-Plot for Table 1 values

The segmentation task is initially executed on an axial plane and then extended to other 2D planes considered in this work. Table 2 to 4 shows the overall eminence of CNN scheme on different 2D slices considered in this research. Table 2 presents the axial-plane result, and the overall performance of this study is presented in Figure 6 using a spider plot. This confirms that the performance metrics by VGG-SegNet are better than other methods.

Similar results are achieved for other 2D planes, and these information are tabulated in Table 3 and Table 4. This substantiates that the proposed scheme with VGG-SegNet attains superior outcome than other CNN schemes.

Table 2. Average performance measures achieved with axial-plane lung CT slices

Image	JA	DI	AC	PR	SE	SP
UNet	89.9037	92.7496	96.8814	92.3820	93.2793	98.9026
ResUNet	89.5944	92.2971	95.9048	92.0365	93.1937	98.5506
VGG-UNet	90.0846	93.8816	97.0366	93.2245	93.3871	99.0078
SegNet	88.4765	92.5407	96.1078	92.2027	93.1664	98.7424
VGG-SegNet	90.1106	94.0910	97.3927	93.5063	93.7163	99.1972

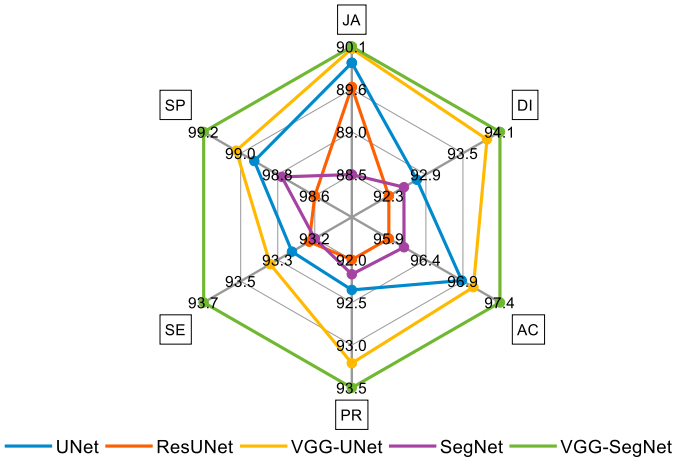

Fig. 6. Spider-plot constructed using the Table 2 information

Table 3. Average performance measures achieved with coronal-plane lung CT slices

Image	JA	DI	AC	PR	SE	SP
UNet	86.8873	91.7075	95.1639	92.1104	92.2917	97.9992
ResUNet	86.3265	91.5207	95.0058	92.1062	92.1148	97.8469
VGG-UNet	88.1074	93.2624	96.5513	93.4783	93.0947	98.2864
SegNet	86.6359	91.3133	95.0582	92.0935	92.1173	97.8996
VGG-SegNet	88.2755	93.3384	96.8173	93.5063	93.2964	98.7399

Table 4. Average performance measures achieved with sagittal-plane lung CT slices

Image	JA	DI	AC	PR	SE	SP
UNet	87.7508	92.8758	96.1847	92.3384	92.7753	98.1947
ResUNet	87.6903	92.5845	96.0639	92.2291	92.5926	98.1284
VGG-UNet	87.9844	93.1159	96.2866	92.5093	93.0884	98.3473
SegNet	87.6538	92.5576	96.0308	92.1899	92.5494	98.1008
VGG-SegNet	88.0754	93.1874	96.3227	92.6497	93.1064	98.5535

5. Conclusion

Automatic disease detection using the chosen biomedical image is widely performed, and the doctors verify and confirm the attained results. This work proposed a CNN segmentation methodology to extort the lung nodule from the CT scan slices. Furthermore, this work implements a two-fold training procedure to improve segmentation accuracy. This framework is tested and validated using the lung CT of different 2D planes, and the result achieved with VGG-SoftMax is better than other schemes in this study. In the future, this two-step training can be implemented on clinically collected lung CT slices.

References

[1] Syed H H, Khan, M. A., Tariq, U., Armghan, A., Alenezi, F., Khan, J. A., Rajinikanth, V., 2021. A rapid artificial intelligence-based computer-aided diagnosis system for COVID-19 classification from CT images. Behavioural Neurology 2021. Article ID 2560388. https://doi.org/10.1155/2021/2560388

[2] https://www.who.int/health-topics/cancer#tab=tab_1

[3] Bhandary, A., Prabhu, G. A., Rajinikanth, V., Thanaraj, K. P., Satapathy, S. C., Robbins, D. E., ... Raja, N. S. M., 2020, Deep-learning framework to detect lung abnormality–A study with chest X-Ray and lung CT scan images. Pattern Recognition Letters, 129, 271-278.

[4] Ahuja, S., Panigrahi, B. K., Dey, N., Rajinikanth, V., Gandhi, T. K., 2021. Deep transfer learning-based automated detection of COVID-19 from lung CT scan slices. Applied Intelligence 51(1), 571-585.

[5] Dey, N., Rajinikanth, V., Fong, S. J., Kaiser, M. S., Mahmud, M., 2020. Social group optimization–assisted Kapur's entropy and morphological segmentation for automated detection of COVID-19 infection from computed tomography images. Cognitive Computation, 12(5), 1011-1023.

[6] Rastogi, P., Khanna, K., Singh, V., 2022. LeuFeatx: Deep learning–based feature extractor for the diagnosis of acute leukemia from microscopic images of peripheral blood smear. Computers in Biology and Medicine, 142, 105236.

[7] Singh, V., Asari, V. K., Rajasekaran, R., 2022. A Deep Neural Network for Early Detection and Prediction of Chronic Kidney Disease." Diagnostics, 12(1): 116.

[8] Rastogi, P., Khanna, K., Singh, V., 2022. Gland segmentation in colorectal cancer histopathological images using U-net inspired convolutional network. Neural Computing and Applications, 34(7), 5383-5395.

[9] Kadry, S., Rajinikanth, V., Taniar, D., Damaševičius, R., Valencia, X. P. B., 2022. Automated segmentation of leukocyte from hematological images—A study using various CNN schemes. The Journal of Supercomputing 78(5): 6974-6994.

[10] Kadry, S., Taniar, D., Damaševičius, R., Rajinikanth, V., Lawal, I. A., 2021. Extraction of abnormal skin lesion from dermoscopy image using VGG-SegNet. In 2021 Seventh International conference on Bio Signals, Images, and Instrumentation (ICBSII), IEEE, 1-5. DOI: 10.1109/ICBSII51839.2021.9445180

[11] Kadry, S., Al-Turjman, F., Rajinikanth, V., 2020. Automated segmentation of COVID-19 lesion from lung CT images using U-Net architecture." In International Summit Smart City 360° 372, 20-30. https://doi.org/10.1007/978-3-030-76063-2_2

[12] Daniel, J., Rose, J. T., Vinnarasi, F., Rajinikanth, V., 2022. VGG-UNet/VGG-SegNet supported automatic segmentation of endoplasmic reticulum network in fluorescence microscopy images. Scanning 2022: Article ID 7733860. https://doi.org/10.1155/2022/7733860.

[13] Das, A., 2022. Adaptive UNet-based lung segmentation and ensemble learning with CNN-based deep features for automated COVID-19 diagnosis." Multimedia Tools and Applications 81(4), 5407-5441.

[14] Khan, M. A., Rajinikanth, V., Satapathy, S. C., Taniar, D., Mohanty, J. R., Tariq, U., and Damaševičius, R. (2021) "VGG19 network assisted joint segmentation and classification of lung nodules in CT images. Diagnostics 11(12), 2208.

[15] Kadry, S., Damaševičius, R., Taniar, D., Rajinikanth, V., Lawal, I. A., 2021. U-net supported segmentation of ischemic-stroke-lesion from brain MRI slices." In 2021 Seventh International conference on Bio Signals, Images, and Instrumentation (ICBSII), IEEE, 1-5. DOI: 10.1109/ICBSII51839.2021.9445126

[16] Krishnamoorthy, S., Zhang, Y., Kadry, S., Yu, W., 2022. Framework to Segment and Evaluate Multiple Sclerosis Lesion in MRI Slices Using VGG-UNet." Computational Intelligence and Neuroscience 2022, Article ID 4928096. https://doi.org/10.1155/2022/4928096

[17] Minaee, S., Boykov, Y. Y., Porikli, F., Plaza, A. J., Kehtarnavaz, N., Terzopoulos,, D., 2021. Image segmentation using deep learning: A survey., IEEE transactions on pattern analysis and machine intelligence 44(7), 3523 – 3542.

[18] http://www.itksnap.org/pmwiki/pmwiki.php

[19] Paul A. Yushkevich, Joseph Piven, Heather Cody Hazlett, Rachel Gimpel Smith, Sean Ho, James C. Gee, Guido Gerig., 2006. User-guided 3D active contour segmentation of anatomical structures: Significantly improved efficiency and reliability. Neuroimage 31(3), 1116-28.

[20] Jain, D., Singh, V., 2018. Diagnosis of breast cancer and diabetes using hybrid feature selection method. In 2018 Fifth International Conference on Parallel, Distributed and Grid Computing (PDGC), IEEE, 64-69. DOI: 10.1109/PDGC.2018.8745830

[21] Vijayakumar, K., Rajinikanth, V., Kirubakaran, M. K., 2022. "Automatic detection of breast cancer in ultrasound images using Mayfly algorithm optimized handcrafted features. Journal of X-Ray Science and Technology, 1-16. DOI: 10.3233/XST-221136

[22] Kadry, S., Rajinikanth, V., González Crespo, R., Verdú, E. (2022). Automated detection of age-related macular degeneration using a pre-trained deep-learning scheme. The Journal of Supercomputing 78(5), 7321-7340.

[23] Diaz, M., Crispo, G., Parziale, A., Marcelli, A., Ferrer, M. A., 2022. Writing Order Recovery in Complex and Long Static Handwriting." International Journal Of Interactive Multimedia And Artificial Intelligence **7(Regular Issue)**: 171-184. http://doi.org/10.9781/ijimai.2021.04.003

[24] Laishram, A., Thongam, K., 2022. Automatic Classification of Oral Pathologies Using Orthopantomogram Radiography Images Based on Convolutional Neural Network." International Journal Of Interactive Multimedia And Artificial Intelligence **7(Regular Issue)**: 69-77. http://doi.org/10.9781/ijimai.2021.10.009